Inorganic Chemistry

Article

pubs.acs.org/IC

Single-Molecule Magnet Behavior and Magnetocaloric Effect in Ferromagnetically Coupled Ln^{III}-Ni^{II}-Ni^{II}-Ln^{III} (Ln^{III} = Dy^{III} and Gd^{III}) Linear Complexes†

Carlos Meseguer,[‡] Silvia Titos-Padilla,[‡] Mikko M. Hänninen,[§] R. Navarrete,[▽] A. J. Mota,[‡] Marco Evangelisti,[⊥] José Ruiz,[‡] and Enrique Colacio*[,‡]

[‡]Departamento de Química Inorgánica, Facultad de Ciencias, Universidad de Granada, Avenida de Fuentenueva s/n, 18071 Granada, Spain

[§]Department of Chemistry, University of Jyväskylä, P.O. Box 35, 40014 Jyväskylä, Finland

[▽]Departamento de Química Inorgánica, Facultad de Farmacia, Universidad de Granada, Campus de Cartuja, 18071 Granada, Spain

[⊥]Instituto de Ciencia de Materiales de Aragón (ICMA), Departamento de Física de la Materia Condensada, CSIC-Universidad de Zaragoza, 50009 Zaragoza, Spain

Supporting Information

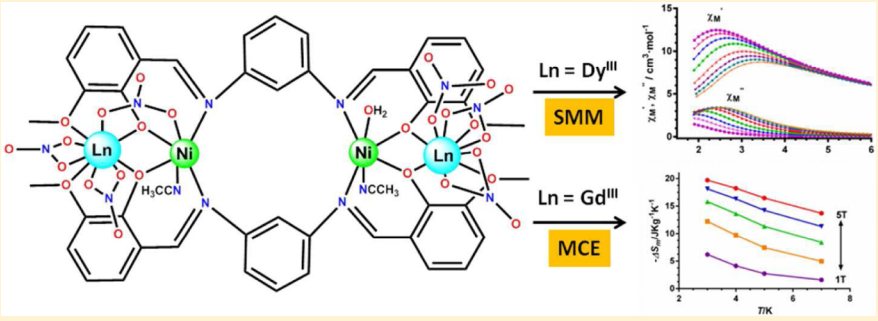

ABSTRACT: New types of linear tetranuclear Ln^{III}-Ni^{II}-Ni^{II}-Ln^{III} (Ln^{III} = Dy (**1**), Gd (**2**)) complexes have been prepared using the multidentate ligand *N*,*N*′-bis(3-methoxysalicylidene)-1,3-diaminobenzene, which has two sets of NO and OO′ coordination pockets that are able to selectively accommodate Ni^{II} and Ln^{III} ions, respectively. The X-ray structure analysis reveals that the Ni^{II} ions are bridged by phenylenediimine groups forming a 12-membered metallacycle in the central body of the complex, whereas the Ln^{III} ions are located at both sides of the metallacycle and linked to the Ni^{II} ions by diphenoxo bridging groups. Phenylenediimine and diphenoxo bridging groups transmit ferromagnetic exchange interactions between the two Ni^{II} ions and between the Ni^{II} and the Ln^{III} ions, respectively. Complex **1** shows slow relaxation of the magnetization at zero field and a thermal energy barrier U_{eff} = 7.4 K with H_{DC} = 1000 Oe, whereas complex **2** exhibits an S = 9 ground state and significant magnetocaloric effect ($-\Delta S_m$ = 18.5 J kg^{-1} K^{-1} at T = 3 K and ΔB = 5 T).

INTRODUCTION

In recent years, the area of molecular magnetism based on heterometallic 3d−4f complexes has undergone a renaissance with the discovery that many of these systems can behave as single-molecule magnets (SMMs)[1] or low-temperature molecular magnetic coolers (MMCs).[2] SMMs exhibit slow relaxation of the magnetization and magnetic hysteresis below a blocking temperature (T_B)[3] and have been proposed as potential candidates for applications in molecular spintronics, ultrahigh density magnetic information storage, and quantum computing at the molecular level.[4] The SMM behavior is due to the existence of an energy barrier (U) that prevents reversal of the magnetization when the magnetic field is brought to zero, leading to bistability of the ground state.[3] MMCs, in turn, exhibit an enhanced magnetocaloric effect (MCE); that is, the change of magnetic entropy (ΔS_m) and adiabatic temperature provoked by the change of an applied magnetic field, which can be potentially used for cryogenic applications.[2,5] Thus, these systems have been proposed as possible alternatives to very-low-temperature technologies and for cryogenic sensors in aerospace devices.[2,5]

Both SMMs and MMCs require large multiplicity in the ground state, which can be guaranteed in the 3d−4f systems by the presence of the lanthanide ion. However, the anisotropy of the system plays a completely different role in SMMs and MMCs. While MMCs should possess a ground state with negligible anisotropy, SMMs require a highly anisotropic ground state, since the height of the energy barrier for the relaxation of the magnetization is dependent on the anisotropy

Received: August 5, 2014
Published: October 28, 2014

   dx.doi.org/10.1021/ic501915j | *Inorg. Chem.* 2014, 53, 12092−12099

of the state. It should be noted that the 3d−4f magnetic exchange interactions are very weak, because of the very efficient shielding of the 4f orbitals of the Ln^{III} ion by the fully occupied 5s and 5p orbitals, and, for the second half of the lanthanide series, these interactions are generally ferromagnetic in nature.[6] Therefore, ground states with large spin multiplicity, as well as multiple low-lying excited and field-accessible states are generated, each of which can contribute to the magnetic entropy of the system enhancing the MCE. Moreover, it is worth mentioning that a large MCE can only be observed when the 3d−4f complex possesses a small molar mass with a large metal/ligand mass ratio, in order to limit the amount of passive, nonmagnetic elements.[4,7] Taking into account the above considerations, small 3d−4f complexes, containing highly anisotropic Dy^{III} ions, could be, in principle, good candidates to show SMM behavior, while those bearing isotropic Gd^{III} ions could exhibit large MCE and, thus, MMC behavior.[4,7] However, it is worth pointing out that SMM and MMC behaviors are closely inter-related to each other, depending on experimental conditions considered, as is particularly evident in the recently investigated GdW_{30} molecule[8] and also illustrated in ref 9.

In recent years, an increasing number of Ni−Dy polynuclear complexes have been reported.[6,10] While only a few of them exhibit SMMs behavior, the MMC properties of their Ni−Gd counterparts have been barely studied.[11] Along these lines, we have exploited the novel ditopic ligand H_2L (*N*,*N*′-bis(3-methoxysalicylidene)-1,3-diaminobenzene), containing two coordination "pockets" (Figure 1) having NO and OO′ donor sets with preference for transition metal and lanthanide ions, respectively, and applied this ancillary in the synthesis of the Ni_2Ln_2 complexes.

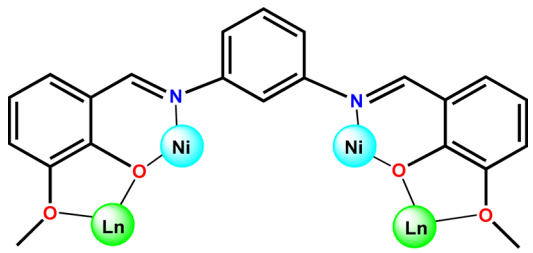

Figure 1. Structure and coordination sites of the ligand H_2L.

Herein, we report the synthesis, X-ray structure and detailed dc/ac magnetic studies of the complexes $[LnNi(H_2O)(CH_3CN)(NO_3)_3(L)NiLn(H_2O)_{0.5}(CH_3CN)(NO_3)_3] \cdot CH_3CN$ (Ln^{III} = Dy (**1**) and Gd (**2**)), complemented with the magnetothermal studies of **2**. Previous results obtained by us and other authors on diphenoxo-bridged Ni^{II}−Gd^{III} complexes[6,10g,l,n,p] and 1,3-phenylendiimine bridged Ni^{II}−Ni^{II} complexes[12] have demonstrated that both types of bridges can facilitate a ferromagnetic interaction. Therefore, these compounds are expected to show ferromagnetic interactions between the metal ions and a high multiplicity in the ground state, which can favor the SMMs behavior in **1** and the existence of a large MCE in **2**. Furthermore, an isostructural Ni_2Y_2 complex containing diamagnetic Y^{III} atoms was prepared to obtain information for the analysis of the magnetic properties of **1** and **2**.

EXPERIMENTAL SECTION

General Procedures. Unless stated otherwise, all reactions were conducted in oven-dried glassware under aerobic conditions, with the reagents purchased commercially and used without further purification. The ligand H_2L was prepared as previously described in the literature.[13]

Preparation of Complexes. *$[Dy_2Ni_2(NO_3)_6(H_2O)_{1.5}(CH_3CN)_2(L)_2]\cdot CH_3CN$ (**1**, Dy_2Ni_2).* To a solution of H_2L (47.5 mg, 0.125 mmol) in 10 mL acetonitrile were subsequently added, with continuous stirring, 36.5 mg (0.125 mmol) of $Ni(NO_3)_2\cdot 6H_2O$ and 56.5 mg (0.125 mmol) of $Dy(NO_3)_3\cdot 5H_2O$ and 36 μL of triethylamine (0.25 mmol). The resulting yellow solution was filtered and allowed to stand at room temperature. After 2 days, well-formed prismatic crystals of compound **1** were obtained in a 55% yield based on Ni. Anal. Calc. For $C_{50}H_{48}Dy_2N_{13}Ni_2O_{27.5}$: C, 35.01; H, 2.82; N, 10.62. Found: C, 35.09; H, 2.75; N, 10.56%. IR (KBr, cm^{-1})): 3350 (m), 1612 (s), 1589 (s), 1560 (s), 1469 (vs), 1382 (vs), 1295 (s), 975 (m), 740 (m).

*$[Gd_2Ni_2(NO_3)_6(H_2O)_{1.5}(CH_3CN)_2(L)_2]\cdot CH_3CN$ (**2**, Gd_2Ni_2).* This compound was prepared in a 60% yield as green crystals, following the procedure for **1**, substituting $Gd(NO_3)_3\cdot 6H_2O$ (59 mg, 0.125 mmol) for $Dy(NO_3)_3\cdot 5H_2O$. Anal. Calc. For $C_{50}H_{48}Gd_2N_{13}Ni_2O_{27.5}$: C, 35.25; H, 2.84; N, 10.70. Found: C, 35.11; H, 2.92; N, 10.79%. IR (KBr, cm^{-1})): 3350 (m), 1612 (s), 1589 (s), 1560 (s), 1469 (vs), 1382 (vs), 1297 (s), 975 (m), 740 (m).

*$[Y_2Ni_2(NO_3)_6(H_2O)_{1.5}(CH_3CN)_2(L)_2]\cdot CH_3CN$ (**3**, Yb_2Ni_2).* This compound was prepared in a 60% yield as green crystals, following the procedure for **1**, substituting $Y(NO_3)_3\cdot 6H_2O$ (49.2 mg, 0.125 mmol) for $Dy(NO_3)_3\cdot 5H_2O$. Anal. Calc. For $C_{50}H_{48}Y_2N_{13}Ni_2O_{27.5}$: C, 38.34; H, 3.09; N, 11.62. Found: C, 38.21; H, 2.98; N, 11.74%. IR (KBr, cm^{-1})): 3350 (m), 1612 (s), 1589 (s), 1560 (s), 1469 (vs), 1382 (vs), 1297 (s), 975 (m), 740 (m).

Physical Measurements. Elemental analyses were carried out at the Centro de Instrumentacion Cientifica (University of Granada) on a Fisons-Carlo Erba analyzer (Model EA 1108). IR spectra on powdered samples were recorded with a Thermo Nicolet IR200FTIR system, using KBr pellets.

Single-Crystal Structure Determination. Data were collected on single crystals of **1** and **2** at 110 K, using a Bruker AXS SMART APEX CCD diffractometer (Mo Kα radiation, λ = 0.71073 Å) outfitted with a CCD area-detector and equipped with an Oxford Cryosystems 700 series Cryostream device. Unit-cell parameters were determined and refined on all observed reflections using APEX2 software.[14] Correction for Lorentz polarization and absorption were applied by SAINT and SADABS programs, respectively.[15,16] Absorption corrections were applied using SADABS.[16] The structures were solved by direct methods and refined by the full-matrix least-squares method on F^2 using the SHELX software suite[17] and the Olex2 program.[18] All non-hydrogen atoms were refined anisotropically. Hydrogen atom positions were calculated and isotropically refined as riding models to their parent atoms. A summary of selected data collection and refinement parameters can be found from the Supporting Information (Table S1).

Magnetic Properties. The variable temperature (2−300 K) magnetic susceptibility measurements under an applied field of 1000 Oe were carried out with a Quantum Design SQUID MPMS XL-5 device. AC magnetic susceptibility measurements

dx.doi.org/10.1021/ic501915j | *Inorg. Chem.* 2014, 53, 12092−12099

in the range of 1−10000 Hz were carried out with a Quantum Design Physical Property Measurement System (PPMS) using an oscillating AC field of 3.5 Oe. The experimental susceptibilities were corrected for the sample holder and diamagnetism of the constituent atoms, using Pascal's tables.

RESULTS AND DISCUSSION

H_2L is a polydentate ligand with bis(NOO′) donor atoms that can also act as a bridge between metal ions through both 1,3-phenylendiimine and phenolate groups. The former one can lead to the formation of Ni_2 metallacycles, whereas the latter can bridge the Ni^{II} and Ln^{III} ions. As expected, the reaction between H_2L and $Ni(NO_3)_2{\cdot}6H_2O$ in acetonitrile, followed by addition of $Ln(NO_3)_3{\cdot}5H_2O$ and triethylamine while using a 1:1:1:2 molar ratio, afforded the tetranuclear Ni_2Ln_2 complexes **1** and **2** in good yield.

Single-crystal X-ray diffraction studies reveal that compounds **1** and **2** are isostructural hence **1** will be used as a representative example to illustrate the common features of the two complexes. The molecular structure of **1** is shown in Figure 2, and comprehensive listing of bond lengths and angles for both **1** and **2** are given in the Supporting Information (Table S2).

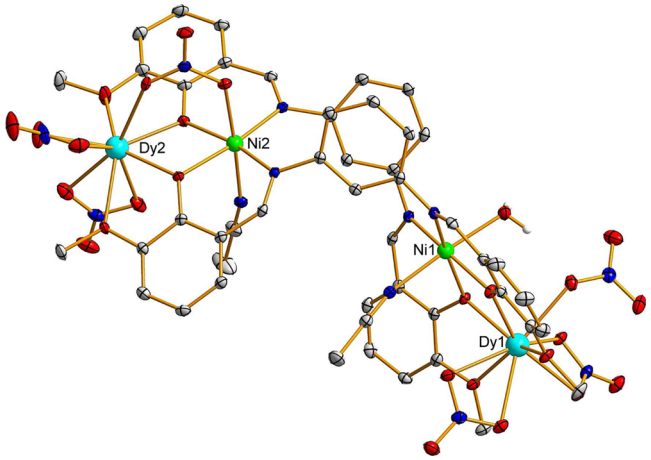

Figure 2. Perspective view of the structure of **1**. Only one of the disordered configurations is represented. Noncoordinated solvents molecules are omitted for clarity.

The solid-state structure of **1** consists of $[Dy_2Ni_2(NO_3)_6(H_2O)_{1.5}(CH_3CN)_2(L)_2]$ molecules of C_1 symmetry with acetonitrile as the solvent of crystallization. The neutral tetranuclear unit can be described as a 12-membered Ni_2 metallacycle with di(*m*-phenylendiimine) bridges connected on both sides to Dy^{III} ions through diphenoxo-bridging groups. The structure is very similar to that previously reported for the complex {[SnBu2][Ni(L)-(NCS)2]}.[19] The Ni^{II} ions exhibit distorted octahedral coordination environments, in which the equatorial plane is composed of two *cis*-imine nitrogens and two phenolato oxygens belonging to pair of fully deprotonated bis(tridentate) L^{2-} bridging ligands. The axial positions are occupied by the nitrogen atom of an acetonitrile and the oxygen atom of a coordinated water molecule. Around the Ni2−Dy2 fragment, the nitrate and water ligands are disordered in the way that one part of the disorder can be refined as a monodentately coordinated nitrate and water molecule as in the Ni1−Dy1 unit, while the other part is formed by bridging nitrate anion (see Figure S1 in the Supporting Information). Hence, other axial position of Ni2 is occupied by either an oxygen from the disordered water molecule or from the bidentate bridging nitrate. The occupation factor ratio between the two parts of the disorder refined very close to 0.5 and was thus fixed into that value (i.e., atoms in both parts are presented in the crystal with an equal occupation of 0.5). The Ni−N_{imine} and Ni−O_{phen} bond distances are in the ranges of 2.092−2.109 Å and 2.028−2.099 Å, respectively, whereas the Ni−N and N−O axial bond distances are 2.072 and 2.095 Å and 2.078 and 2.110 Å, respectively.

The Dy1 atom exhibits a rather nonsymmetrical DyO_9 coordination, which consists of two bridging phenoxo oxygens, two methoxy oxygens, and five oxygen atoms belonging to two bidentate and one monodentate nitrate anions. The Dy2 atom exhibits a similar DyO_9 coordination sphere, which is built, in addition to the phenoxo and methoxy oxygens from the ligand, out of five oxygen atoms belonging to three coordinated nitrate anions (two bidentate and a disordered bridging or monodentate one). In addition to the disorder involving the water molecule and bridging/monodenate nitrate anion (*vide supra*), both bidentately coordinated nitrates can be refined in distinct parts with slightly different terminal positions. The Dy−$O_{phenoxo}$ bond distances in the range of 2.342(2) Å and 2.322(2) Å are shorter than Dy−$O_{nitrate}$ and Dy−$O_{methoxy}$ bond lengths in the ranges of 2.492(2)−2.522(2) Å and 2.608(2)−2.564(2) Å, respectively, thus indicating a high degree of asymmetry in the DyO_9 coordination spheres. In fact, the calculation of the degree of distortion of the Dy coordination polyhedra with respect to the ideal nine-vertex polyhedra, by using the continuous shape measure theory and SHAPE software,[20] indicated that the lower values of the shape measures were those relative to the muffin (C_s), spherical capped square antiprism (C_{4v}), spherical tricapped trigonal prism (D_{3h}) (1.90, 2.43, and 2.26, respectively, for Dy1, 2.35, 2.49, and 2.22, respectively, for Dy2 with the monodentate nitrate anion and 2.39, 3.03, and 4.06, respectively, for Dy2 with the bridging nitrate). Therefore, the DyO_9 coordination sphere can be considered as intermediate between all these nine-vertex polyhedra. The shape measures relative to other reference polyhedra are significantly larger (see Table S3 in the Supporting Information).

The Ni(μ-O_2)Dy bridging fragments are almost planar with a hinge angles of 177.8(1)° and 172.1(1)° (dihedral angle between the O−Ni−O and O−Dy−O planes) for Dy1 and Dy2, respectively, and rather symmetric average Ni−O−Dy bridging angles of 105.1° and 106.3°. The Ni1···Dy1 and Ni2···Dy2 separations are 3.489(1) Å and 3.437(1) Å, whereas the Ni···Ni distance is 6.889(1) Å. The angles between the bridging phenylene rings and the NiN_2O_2 equatorial coordination planes of Ni1 and Ni2 are 57.1° and 66.0°, and 60.6° and 69.7°, respectively. The phenylene rings are rotated and slightly tilted each to other with an interplanar distance of 3.302 Å, thus indicating the existence of significant $\pi\cdots\pi$ interactions.

Despite a large interest in 3d/4f complexes, only a few examples of tetranuclear $Ni^{II}_2Ln_2^{III}$ complexes have been reported so far,[8j,8q,21] and to the best of our knowledge, complexes **1** and **2** represent the first reported examples of linear Ln^{III}-Ni^{II}-Ni^{II}-Ln^{III} species.

Magnetic Properties. The magnetic properties of **1** and **2** were measured on polycrystalline samples in the 2−300 K temperature range under an applied magnetic field of 0.1 T and

dx.doi.org/10.1021/ic501915j | Inorg. Chem. 2014, 53, 12092−12099

the data are given in Figure 3 in the form $\chi_M T$ vs T (where χ_M is the magnetic susceptibility per $Ni^{II}_2Ln^{III}_2$ unit).

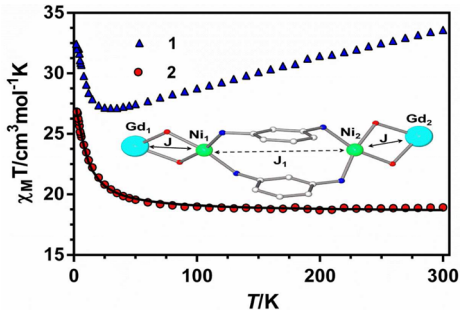

Figure 3. Temperature dependence of the $\chi_M T$ for **1** and **2**. Solid line represents the best fit of the experimental data of **2** with the Hamiltonian described by eq 1 (presented later in this work).

Dy_2Ni_2 (1). At room temperature, the $\chi_M T$ product of **1** (33.6 cm^3 K mol^{-1}) is close to the calculated value for independent Ni^{II} (S = 1 with g_{Ni} = 2.0) and Dy^{III} ions ($^6H_{15/2}$, g_J = 4/3) in the free-ion approximation (30.34 cm^3 K mol^{-1}). The $\chi_M T$ value for **1** decreases slowly with decreasing temperature, reaching a minimum at ∼30 K with a value of 27.14 cm^3 K mol^{-1}. This behavior is due to depopulation of the m_j sublevels of the Dy^{III} ion, which arise from the splitting of the ground $^6H_{15/2}$ multiplet by the ligand field. Below this temperature, $\chi_M T$ increases to reach a value of 32.44 cm^3 K mol^{-1} at 2 K. This increase in $\chi_M T$ at temperatures below ∼30 K is due to a ferromagnetic interaction between Ni^{II} and Dy^{III}.

The M vs H plot at 2 K for **1** (see Figure S2 in the Supporting Information) shows a relatively rapid increase in the magnetization at low field, in accordance with the high-spin state for this complex, and then a linear increase without achieving a complete saturation at 5 T. The linear high-field variation of the magnetization suggests the presence of a significant magnetic anisotropy and/or low-lying excited states that are partially populated. It should be noted that the magnetization value for **1** at 5 T (14.35 $N\mu_B$) is far from the saturation values expected for two Dy^{III} ions ferromagnetically coupled with two S_{Ni} = 1 (24 $N\mu_B$); this is due to the splitting of the ground-state multiplet of the Dy^{III} ion promoted by the crystal-field effects (the value of saturation magnetization for mononuclear Dy^{III} complexes is ∼5 $N\mu_B$).[22]

Dynamic AC magnetic susceptibility measurements, as a function of the temperature and frequency, for **1** are given in Figure 4 and Figure S3 in the Supporting Information, respectively. Dynamic AC magnetic susceptibility measurements, as a function of the temperature under zero-external applied DC field, show a frequency dependency of the in-phase (χ'_M) and out-of-phase (χ''_M) signals (Figure 4). This behavior seems to indicate slow relaxation of the magnetization, which is typical for a SMM. However, there is no clear maximum in the temperature dependence of χ''_M above 2 K, at frequencies reaching 10 000 Hz. This feature could be due either to the existence of fast resonant zero-field quantum tunneling of the magnetization (QTM) through degenerate energy levels or to a very small energy barrier. The QTM relaxation process is forbidden for Kramers doublets (the zero-field tunnel splitting is zero), but could be made possible by dipolar and/or hyperfine interactions. When the AC measurements were performed in the presence of a small external DC field of 1000 G to fully or partly suppress the quantum tunneling relaxation, compound **1** showed slow relaxation of the magnetization with clear maxima in the χ''_M vs T curves, which appear in the range between 2.0 K (1000 Hz) and 2.61 K (10000 Hz) (Figure 4).

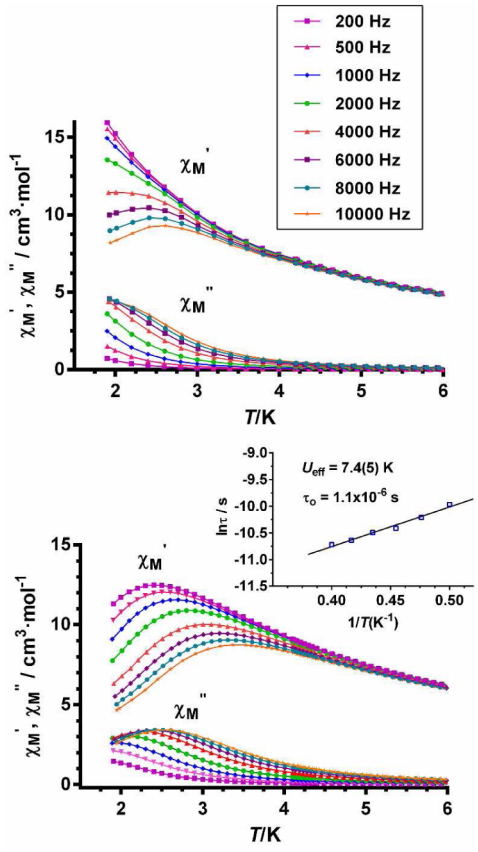

Figure 4. In-phase (χ'_M) and out-of-phase (χ''_M) signals under zero (top) and 1000 Oe (bottom) DC fields and Arrhenius plot (inset) for **1**.

The Cole−Cole diagrams in the temperature range of 2−2.8 K (Figure S4 in the Supporting Information) exhibit semicircular shapes and can be fitted using the generalized Debye model, affording α values in the range of 0.23−0.37, which supports the existence of a broad distribution of relaxation times. The set χ_0 (isothermal susceptibility), χ_S (adiabatic susceptibility), and α obtained in the above fits were further used to fit the frequency dependence of χ''_M at each temperature to the generalized Debye model, which permits the relaxation time τ to be extracted. The results were then used to construct the Arrhenius plot shown in Figure 4. The linear fit of the data (τ vs $1/T$) afforded an effective energy barrier for the reversal of the magnetization of U_{eff} = 7.4(5) K with $\tau_o = 1.1 \times 10^{-6}$ s. The fact that the isostructural Ni_2Y_2 complex does not exhibit slow relaxation of the magnetization above 2 K, points out that the SMM behavior found for **1** arises from the presence of the Dy^{III} ions.

At this point, note that Ln^{III}-Ni^{II} polynuclear complexes are attracting much attention in the field of SMMs, because the combination of Ln^{III} ions with strong magnetic anisotropy and Ni^{II} ions with second-order magnetic anisotropy could lead to improved SMMs properties. Despite this observation, only a few examples of Ni-Ln complexes (with paramagnetic Ni^{II} ions) exhibiting SMM behavior have been reported so far.[6,10] Most of them are field-induced SMMs and, to the best of our

dx.doi.org/10.1021/ic501915j | Inorg. Chem. 2014, 53, 12092−12099

knowledge, SMM behavior was observed under zero field with maxima in the AC out-of-phase peaks above 2 K in only six instances,[10o−t] which exhibit relatively small energy barriers. Among them, the defective dicubane complexes Ni_4Ln_2 (Ln = Tb^{III}, Dy^{III}) present the highest thermal energy barriers reported so far, with U_{eff} values of 30 and 32 K, respectively.[10t] The small energy barrier observed for **1** and other Ni−Dy-based SMMs could be due, among other reasons, to (i) a weak anisotropy for the entire molecule and (ii) the weak magnetic exchange coupling between Ni^{II} and Dy^{III} ions, leading to a small energy separation between the ground state and the first excited state, which determine the value of U_{eff}. With regard to point (i), either low anisotropy of the Dy^{III} ions induced by the ligand-field effects or the different relative orientation of the local anisotropic axes of the Ni^{II} and Dy^{III} ions could lead to a relatively low anisotropy of the entire molecule. With regard to point (ii), the Ni−Dy interactions generally are weaker than the Ni−Gd ones and, therefore, a J_{NiDy} value of <2 cm^{-1} is expected for **1** (see below). For such a J value, the first excited state is only a few wavenumbers above the ground state and, therefore, the thermal energy barrier would be small. In addition, since the Ni−Dy interaction is weak, the Ni^{II} ions can have independently reorienting magnetic moments at T = 2 K, so that they act as sources of random magnetic field for the Dy^{III} ions, thus favoring a quantum tunneling splitting that diminishes the thermal energy barrier.[23] The fact that the Ni_3Dy_2 pentanuclear complex recently reported by Chadrasekhar et al.,[24] in which the Ni^{II} ions are diamagnetic, exhibits the highest energy barrier ever found for a Ni−Dy system (U_{eff} = 85 K), supports our hypothesis that weak Dy−Ni interactions lead to a small gap between the ground and first excited states and, thus, to small energy barriers. In good accord with this hypothesis, the N_2^{3-} radical bridged dinuclear complex, [K(18-crown-6)]{[$(Me_3Si)_2N$]$_2$(THF)Dy}$_2$(μ-η2:η2-N2),[25] which possesses a very important magnetic exchange interaction between the radical and the Dy^{III} ions, exhibits a very large anisotropy barrier (U_{eff} = 123 cm^{-1}). However, the nonradical N_2^{2-}-bridged analogue,[25] which possesses a very weak magnetic exchange interaction between the Dy^{III}, shows a drastic reduction of the anisotropy barrier to U_{eff} = 18 cm^{-1}. These results highlight the essential role played by the magnetic exchange interaction in determining the magnitude of the anisotropy barrier in lanthanide-containing polynuclear complexes.

In view of the above considerations, the approach of introducing several anisotropic metal ions in a polynuclear complex, as in **1**, may not have a positive effect on the SMM behavior. In connection with this, Chibotaru et al.[26] have recently suggested, from theoretical studies, that a better strategy to obtain efficient SMMs systems would be that of combining strong anisotropic metal ions with large angular momentum and isotropic metal ions with large spin momentum such as Gd^{III}.

*Gd_2Ni_2 (**2**).* The room-temperature $\chi_M T$ value for **2** of 18.92 cm^3 K mol^{-1} is slightly higher but still in relative good agreement with the expected value for a couple of Ni^{II} (S = 1) and a couple of Gd^{III} (S = 7/2) noninteracting ions (17.75 cm^3 K mol^{-1} with g = 2). Upon lowering the temperature from room temperature to 50 K, the $\chi_M T$ value slowly increases (19.55 cm^3 K mol^{-1}) and then in a more abrupt way to reach a value of 26.82 cm^3 K mol^{-1} at 2.5 K (Figure 3). This behavior is due to Ni^{II}−Gd^{III} and Ni^{II}−Ni^{II} ferromagnetic interactions through the diphenoxo and diphenylenediimine bridging groups leading to a S_T = 9 ground spin state.[21] The magnetic properties of **2** have been modeled using the following Hamiltonian:

$$\hat{H} = -J(\hat{S}_{Ni1}\hat{S}_{Gd1} + \hat{S}_{Ni2}\hat{S}_{Gd2}) - J_1(\hat{S}_{Ni1}\hat{S}_{Ni2}) + D_{Ni}\sum_{i=1}^{2}(\hat{S}_{zi}^{\,2} - S_i(S_i+1)/3) \quad (1)$$

where J and J_1 account for the magnetic exchange coupling between Ni^{II} and Gd^{III} ions through the diphenoxo bridging group and between the Ni^{II} ions, through the diphenylenediimine bridging group, respectively, and D_{Ni1} is the axial single ion zero-field parameter of the Ni^{II} ions. Although there are small differences between the bond angles and distances affecting the two halves of the molecule, for the sake of simplicity, we are going to consider the same exchange coupling for the two Ni^{II}−Gd^{III} interactions. Note that J_1 and D_{Ni} show a positive correlation, so that D_{Ni} increases as J_1 increases. In view of this, we decided to study the magnetic properties (see Figure S5 in the Supporting Information) of the isostructural Ni_2Y_2 complex (**3**) to get an estimate of the zero-field splitting parameter (D_{Ni}) and to confirm the nature of the magnetic exchange interaction mediated by the phenylenediimine bridge (J_1). Even though we have not been able to obtain single crystals of **3** of sufficiently high quality to determine the molecular structure, elemental analyses, infrared (IR) spectra, and powder X-ray diffraction (XRD) data clearly indicate that all three complexes are isostructural (see Figures S6 and S7 in the Supporting Information). The $\chi_M T$ product for **3** at room temperature (2.17 cm^3 K mol^{-1}) is close to that expected for two noninteracting Ni^{II} ions with g = 2 (2.0 cm^3 K mol^{-1}). The $\chi_M T$ product slowly increases as the temperature decreases from 300 K to 15 K (2.195 cm^3 K mol^{-1}) and then sharply decreases to 1.40 cm^3 K mol^{-1} at 2 K. The increase observed in the temperature range of 300−15 K is due to a very weak ferromagnetic interaction between the Ni^{II} ions, whereas the decrease at low temperature can be due to different factors, such as the existence of intermolecular antiferromagnetic interactions between Ni_2Y_2 and zero-field splitting effects of the Ni^{II} ions. Since the molecules are well-isolated in the crystal, we believe that the decrease in $\chi_M T$ at low temperature is mainly due to the latter factor. Hence, we have modeled the magnetic properties of **3** with the following Hamiltonian:

$$\hat{H} = -J_1(\hat{S}_{Ni1}\hat{S}_{Ni2}) + D_{Ni}\sum_{i=1}^{2}(\hat{S}_{zi}^{\,2} - S_i(S_i+1)/3) \quad (2)$$

where J_1 and D_{Ni} account for the magnetic exchange coupling between Ni^{II} ions and the axial single ion zero-field splitting parameter of the Ni^{II} ion, respectively. Simultaneous fitting of $\chi_M T$ vs T and the M versus field at 2 K with the above Hamiltonian with the PHI program[27] (using a mean g value to avoid overparameterization) afforded the following set of parameters: J_1 = +0.38 cm^{-1}, g = 2.08, D_{Ni} = 4.63 cm^{-1} and $R = 1.5 \times 10^{-6}$ ($R = \sum(\chi_M T_{calc} - \chi_M T_{exp})^2/\sum(\chi_M T_{exp})^2$). The D_{Ni} values are in agreement with the expected single-ion values reported in the literature.[28]

The D_{Ni} value extracted for compound **3** was used as a fixed parameter in the fitting of the magnetic data of **2** with the Hamiltonian given in eq 1. The simultaneous fitting of the $\chi_M T$ vs T (Figure 3) and the M vs field plots (Figure 5) allowed the extraction of the following parameters: J = +1.80 cm^{-1}, J_1 = +0.42 cm^{-1}, g = 2.04, and $R = 4.2 \times 10^{-5}$ (with a fixed D = 4.63

dx.doi.org/10.1021/ic501915j | Inorg. Chem. 2014, 53, 12092−12099

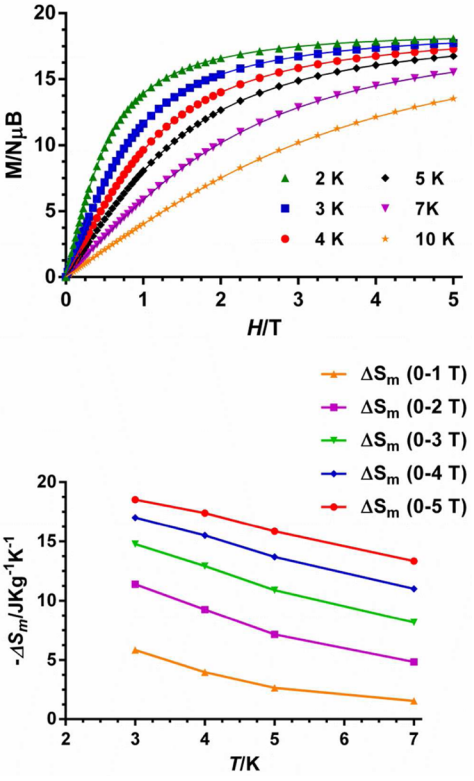

Figure 5. Field dependence of the magnetization plots for **2** between 2 and 10 K (top) and magnetic entropy changes ($-\Delta S_m$) calculated using the magnetization data for **2** from 1 T to 5 T and temperatures from 3 K to 7 K (bottom).

cm^{-1}). When D is fixed to zero, the same values are obtained for J and g, but J_1 decreases to a value of +0.23 cm^{-1} with $R = 4.3 \times 10^{-5}$.

Theoretical calculations carried out on diphenoxo bridged NiGd[2b,6,29] complexes have shown that the ferromagnetic interaction between the Ni^{II} and Gd^{III} ions increases with the increase of θ (Ni−O−Gd bridging angle) and with the decrease of β (the hinge dihedral angle between the O−Ni−O and O−Gd−O planes), although the former angle plays a major role in determining the value of J. The experimental J values for diphenoxo-bridged Ni−Gd dinuclear complexes given in Table 1 are in good accord with these magneto-structural correlations. As can be observed in this table, Ni−Gd complexes having structural parameters similar to those of **2**, that is to say, almost planar systems ($\beta \approx 0$) and θ angles of ∼106°, present J values of approximately +2 cm^{-1}, which are very close to that found for **2**.

As far as we know, no examples of magnetically characterized Ni^{II} dinuclear complexes with Schiff base ligands containing 1,3-phenylenediimine bridging fragment have been reported so far. However, results for dinuclear Cu_2 complexes with these types of ligand show ferromagnetic interactions and, in one instance, antiferromagnetic coupling.[13,30] It has been proposed that the nature and magnitude of the magnetic coupling depends on the substituents attached to the backbone of the ligand.[30] Interestingly, triple stranded Ni_2 complexes with 1,3-bis(pyridine-2-carboxamide)benzene bearing the 1,3-phenylenediamine bridging fragment exhibit weak ferromagnetic interactions.[12b,c] In view of the above-reported results, it would be reasonable to assume that the J_{NiNi} interaction through the 1,3-phenylenediimine bridging fragment should be ferromagnetic in nature. Nevertheless, in order to support the experimental values of the J_{NiGd} interaction and fundamentally the ferromagnetic nature of the J_{NiNi} interaction through the 1,3-phenylenediimine bridging fragment, we have performed DFT calculations on the X-ray structures as found in the solid state. The calculated J_{Ni1Gd1} and J_{Ni2Gd2} (structural parameters for both halves of the molecule are slightly different) are +3.39 and +3.33 cm^{-1}, respectively, whereas the calculated J_{Ni2Ni2} is +1.35 cm^{-1}), which agree in sign and rather well in magnitude with the corresponding experimental parameters. The difference between the experimental and calculated values could be due to limitations inherent to the method as well as being due to the fact that the experimental J values include the Gd_2−Ni_1, Gd_1−Ni_2 and Gd_1−Gd_2 coupling constants, which have been calculated to be antiferromagnetic in nature, with non-negligible J values of −0.44, −0.58, and −0.12 cm^{-1}, respectively.

The magnetothermal properties of **2** were studied since the observed ferromagnetic interactions between the Gd^{III} and Ni^{II} ions and between the Ni^{II} ions induce a large total spin ground state ($S = 9$) but also because Gd^{III} ions are isotropic and Ni^{II}, although anisotropic, possess only second-order anisotropy. Therefore, a relatively significant magnetocaloric effect is expected for **2**. The magnetic entropy changes ($-\Delta S_m$) that characterize the magnetocaloric properties of **2** can be calculated from the experimental isothermal field-dependent magnetization data (Figure 5) by using the Maxwell relation:

$$\Delta S_m(T, \Delta B) = \int_{B_i}^{B_f} \left[\frac{\partial M(T, B)}{\partial T}\right]_B dB$$

Table 1. Magnetostructural Data for Diphenoxo Bridged Dinuclear NiGd Complexes

complex	J_{exp} (cm^{-1})	θ (deg)[a]	β (deg)[a]	Gd···Ni[a] (Å)	ref
$[Ni(H_2O)(\mu\text{-}L^1)Ln(NO_3)_3]\cdot 2CH_3OH$	+2.16	109.4	2.3	3.565	6
$[L^2Ni(H_2O)_2Gd(NO_3)_3]$	+3.6	107.2	2.8	3.522	10a
$[Ni(CH_3CN)_2(valpan)Gd(NO_3)_3]\cdot CH_3CN$	+2.3	106.1	0.22	3.467	10g
$[Ni(\mu\text{-}L^1)(\mu\text{-}Ac)Gd(NO_3)_2]$	+1.38	104.4	21.4	3.456	6
[Ni(valpan)(MeOH)(ac)Ln(hfac)$_2$]	+2.2	102.1	13.5	3.384	10l
$[(H_2O)Ni(ovan)_2(\mu\text{-}NO_3)Gd(ovan)(NO_3)_2]H_2O$	+1.36[b]	101.6	0.8	3.324	10e
$[L^3Ni(H_2O)(\mu\text{-}OAc)Ln(NO_3)_2]\cdot CH_3CN$	+1.54	103.3	14.8	3.443	10n

[a]Average values. [b]No available structural data and those included in the table correspond to the YNi_2 isostructural complex: H_2L^1 = *N,N′,N″*-trimethyl-*N,N″*-bis(2-hydroxy-3-methoxy-5-methylbenzyl)diethylenetriamine; H_2L^2 = *N,N*-2,2-dimethylpropylenedi(3-methoxysalicylideneiminato); valpan = *N,N*-propylenedi(3-methoxysalicylideneiminato); ovan = *o*-vanillin; Schiff-base resulting from the 1:2 condensation of 1,1′-diacetylferrocene dihydrazone and *o*-vanillin. θ is the Ni−O−Gd bridging angle and β is the dihedral angle between the O−Ni−O and O−Ln−O planes in the bridging fragment. [c]There are two J_{NiGd} as the $GdNi_2$ trinuclear complex is not centrosymmetric.

dx.doi.org/10.1021/ic501915j | Inorg. Chem. 2014, 53, 12092−12099

where B_i and B_f are the initial and final applied magnetic fields. The values of $-\Delta S_m$ for **2** under all fields increase as the temperature decreases from 7 K to 3 K. The maximum value of $-\Delta S_m$ achieved for **2** is 18.5 J kg^{-1} K^{-1} at T = 3 K with a change in applied field of ΔB = 5 T (Figure 5). Despite the Ni^{II} anisotropy, there is significant change in the $-\Delta S_m$ for **2**, which is consistent with the easy spin polarization in relatively weak magnetic fields. It should be noted that $-\Delta S_m$ could not be determined below 2 K, because of the limitations of our instrument, although it is expected to increase further with decreasing temperature. We have also simulated the MCE for **2**, using the magnetic parameters extracted when D was fixed to zero (see Figure S8 in the Supporting Information). The obtained magnetic anisotropy values indicate that the value of $-\Delta S_m$ at 5 T is reduced by 1.2 J kg^{-1} K^{-1} (5.7%) by the Ni^{II} anisotropy.

As expected, the extracted $-\Delta S_m$ value of 18.5 J kg^{-1} K^{-1} at T = 3 K is lower than that calculated for the full magnetic entropy content per mole (i.e., $2R \ln(2S_{Ni} + 1) + 2R \ln(2S_{Gd} + 1) = 6.36R = 31.08$ J kg^{-1} K^{-1}) but it is higher than that expected for a S = 9 Ni_2Gd_2 unit (i.e., $-\Delta S_m = R \ln(2S + 1) = 2.94R = 13.85$ J kg^{-1} K^{-1}). Moreover, the extracted $-\Delta S_m$ value at 5 T is larger than that observed for Ni_2Gd_2[11d] and Ni_2Gd[11i,h] complexes having similar molecular mass, but lower than those found under the same conditions for other more magnetically dense NiGd clusters with Gd/Ni ratios larger than 1[11b−d] and other Gd[31] or 3d−Gd complexes.[32] However, the magnetothermal results for **2** and other small clusters demonstrate that these systems can be a good approach for novel molecular magnetic refrigerants.

CONCLUDING REMARKS

The multidentate ligand *N*,*N*′-bis(3-methoxysalicylidene)-1,3-diaminobenzene, with two sets of symmetrically distributed NO and OO′ coordination pockets flanking the phenyl ring, shows selective preference for Ni^{II} and Ln^{III} ions, respectively, in the preparation of the first examples of structurally and magnetically characterized linear tetranuclear Ln^{III}-Ni^{II}-Ni^{II}-Ln^{III} (Ln^{III} = Dy (**1**), Gd (**2**)) species. The central body of the complexes consists of a 12-membered Ni_2 metallacycle with di(*m*-phenylenediimine) bridges. On both sides of the ring, Dy^{III} ions are connected to Ni^{II} ions through diphenoxo-bridging groups. DC magnetic susceptibility studies indicate the presence of dominant ferromagnetic interactions in both **1** and **2**. Complex **1** shows frequency-dependent out-of-phase AC signals, which is indicative of slow relaxation of the magnetization and potential SMM behavior, whereas complex **2** exhibits a S = 9 ground state and significant MCE. Moreover, the reduction of the MCE effect promoted by the Ni^{II} anisotropy has been quantified to be ∼6%. Currently, we are studying the structurally similar tetranuclear $M_2^{II}Ln^{III}$ (M^{II} = Co, Cu, Zn) complexes with the prospect of evaluating how the anisotropy of the metal ions or the presence of diamagnetic metal ions affect the SMM and magnetothermal properties. The replacement of Ni^{II} by diamagnetic Zn^{II} in these $M_2^{II}Dy^{III}$ complexes is expected to provoke a considerable increase of the effective energy barrier (U_{eff}).

ASSOCIATED CONTENT

Supporting Information

X-ray crystallographic data for **1** and **2**, including data collection, refinement, and selected bond lengths and angles. Shape measures, IR and PXRD data for **1**−**3**, DC susceptibility data for complex **3**, variable-frequency temperature dependence of the AC in-phase χ'_M signal and Cole−Cole plots for complexes **1** and simulation of the MCE effect for **2** with D = 0. This material is available free of charge via the Internet at http://pubs.acs.org.

AUTHOR INFORMATION

Corresponding Author

*E-mail: ecolacio@ugr.es.

Notes

The authors declare no competing financial interest.

ACKNOWLEDGMENTS

Financial support from Ministerio de Economía y Competitividad (MINECO) for Project Nos. CTQ-2011-24478 and MAT2012-38318-C03-01, the Junta de Andalucía (No. FQM-195 and Project of Excellence No. P11-FQM-7756), and the University of Granada are acknowledged. S.T. thanks to Junta de Andalucia for a post-doctoral contract.

DEDICATION

†This paper is dedicated to the memory of the co-authors and our lovely friend, José Ruiz, who recently passed away.

REFERENCES

(1) For some recent reviews, see: (a) Winpenny, R. E. P. *Chem. Soc. Rev.* **1998**, *27*, 447−452. (b) Benelli, C.; Gatteschi, D. *Chem. Rev.* **2002**, *102*, 2369−2388. (c) Sessoli, R.; Powell, A. K. *Coord. Chem. Rev.* **2009**, *253*, 2328−2341. (d) Andruh, M.; Costes, J. P.; Diaz, C.; Gao, S. *Inorg. Chem.* **2009**, *48*, 3342−3359 (Forum Article). (e) *Dalton Trans.* **2010**, *39* ("Molecular Magnets", themed issue; E. K. Brechin, Ed.). (f) Andruh, M. *Chem. Commun.* **2011**, *47*, 3025−3042. (g) Sorace, L.; Benelli, C.; Gatteschi, D. *Chem. Soc. Rev.* **2011**, *40*, 3092−3104.

(2) Some reviews: (a) Evangelisti, M.; Brechin, E. K. *Dalton Trans.* **2010**, *39*, 4672−4676. (b) Cremades, E.; Gomez-Coca, S.; Aravena, D.; Alvarez, S.; Ruiz, E. *J. Am. Chem. Soc.* **2012**, *134*, 10532−10542. (c) Sharples, J. W.; Collison, D. *Polyhedron* **2013**, *54*, 91−103. (d) Zheng, Y.-Z.; Zhou, G.-J.; Zheng, Z.; Winpenny, R. E. P. *Chem. Soc. Rev.* **2014**, *43*, 1462−1475.

(3) Gatteschi, D.; Sessoli, R.; Villain, J. *Molecular Nanomagnets*; Oxford University Press; Oxford, U.K., 2006.

(4) (a) Leuenberger, M. N.; Loss, D. *Nature* **2001**, *410*, 789−793. (b) Rocha, A. R.; García-Suárez, V. M.; Bailey, S. W.; Lambert, C. J.; Ferrerand, J.; Sanvito, S. *Nat. Mater.* **2005**, *4*, 335−339. (c) Ardavan, A.; Rival, O.; Morton, J. J. L.; Blundell, S. J.; Tyryshkin, A. M.; Timco, G. A.; Winpenny, R. E. P. *Phys. Rev. Lett.* **2007**, *98*, 057201. (d) Bogani, L.; Wernsdorfer, W. *Nat. Mater.* **2008**, *7*, 179−186. (e) Affronte, M. *J. Mater. Chem.* **2009**, *19*, 1731−1737. (f) Stamp, P. C. E.; Gaita-Ariño, A. *J. Mater. Chem.* **2009**, *19*, 1718−1730. (g) Candini, A.; Klyatskaya, S.; Ruben, M.; Wernsdorfer, W.; Affronte, M. *Nano Lett.* **2011**, *11*, 2634−2639. (h) Vincent, R.; Klyatskaya, S.; Ruben, M.; Wernsdorfer, W.; Balestro, F. *Nature* **2012**, *488*, 357−360. (i) Ganzhorn, M.; Klyatskaya, S.; Ruben, M.; Wernsdorfer, W. *Nat. Nanotechnol.* **2013**, *8*, 165−169. (j) Jenkins, M.; Hümmer, T.; Martínez-Pérez, M. J.; García-Ripoll, J.; Zueco, D.; Luis, F. *New J. Phys.* **2013**, *15*, 095007.

(5) Sessoli, R. *Angew. Chem., Int. Ed.* **2011**, *50*, 2.

(6) Colacio, E.; Ruiz, J.; Mota, A. J.; Palacios, M. A.; Cremades, E.; Ruiz, E.; White, F. J.; Brechin, E. K. *Inorg. Chem.* **2012**, *51*, 5857−5868.

(7) Colacio, E.; Ruiz, J.; Lorusso, G.; Brechin, E. K.; Evangelisti, M. *Chem. Commun.* **2013**, *49*, 3845−3847.

(8) (a) Martínez-Pérez, M.-J.; Montero, O.; Evangelisti, M.; Luis, F.; Sesé, J.; Cardona-Serra, S.; Coronado, E. *Adv. Mater.* **2012**, *24*, 4301−4305. (b) Martínez-Pérez, M.-J.; Cardona-Serra, S.; Schlegel, C.; Moro, F.; Alonso, P. J.; Prima-García, H.; Clemente-Juan, J. M.; Evangelisti,

M.; Gaita-Ariño, A.; Sesé, J.; Van Slageren, J.; Coronado, E.; Luis, F. *Phys. Rev. Lett.* **2012**, *108*, 247213. (c) Baldoví, J. J.; Cardona-Serra, S.; Clemente-Juan, J. M.; Coronado, E.; Gaita-Ariño, A.; Prima-García, H. *Chem. Commun.* **2013**, *49*, 8922−8924.

(9) Luis, F.; Evangelisti, M. Magnetic refrigeration and spin-lattice relaxation in gadolinium-based molecular nanomagnets. In *Molecular Nanomagnets and Related Phenomena*; Gao, S., Ed.; Springer−Verlag: Berlin, Heidelberg, Germany, 2014.

(10) (a) Costes, J.-P.; Dahan, F.; Dupuis, A.; Laurent, J. P. *Inorg. Chem.* **1997**, *36*, 4284−4286. (b) Chen, Q.-Y.; Luo, Q.-H.; Zheng, L.-M.; Wang, Z.-L.; Chen, J.-T. *Inorg. Chem.* **2002**, *41*, 605−609. (c) Mori, F.; Ishida, T.; Nogami, T. *Polyhedron* **2005**, *24*, 2588−2592. (d) Yamaguchi, T.; Sunatsuki, Y.; Ishida, H.; Kojima, M.; Akashi, H.; Re, N.; Matsumoto, N.; Pochaba, A.; Mrozinski, J. *Inorg. Chem.* **2008**, *47*, 5736−5745. (e) Costes, J.-P.; Vendier, L. *Eur. J. Inorg. Chem.* **2010**, *18*, 2768−2773. (f) Efthymiou, C. G.; Stamatatos, T. C.; Papatriantafyllopoulou, C.; Tasiopoulos, A. J.; Wernsdorfer, W.; Perlepes, S. P.; Christou, G. *Inorg. Chem.* **2010**, *49*, 9737−9739. (g) Pasatoiu, T. D.; Sutter, J.-P.; Madalan, A. M.; Fellah, F. Z. C.; Duhayon, C.; Andruh, M. *Inorg. Chem.* **2011**, *50*, 5890−5898. (h) Cimpoesu, F.; Dahan, F.; Ladeira, S.; Ferbinteanu, M.; Costes, J.-P. *Inorg. Chem.* **2012**, *51*, 11279−11293. (i) Ke, H.; Zhao, L.; Guo, Y.; Tang, J. *Inorg. Chem.* **2012**, *51*, 2699−2705. (j) Abtab, S. M. T.; Maity, M.; Bhattacharya, K.; Sañudo, E. C.; Chaudhury, M. *Inorg. Chem.* **2012**, *51*, 10211−10221. (k) Xiong, K.; Wang, X.; Jiang, F.; Gai, Y.; Xu, W.; Su, K.; Li, X.; Yuana, D.; Hong, M. *Chem. Commun.* **2012**, *48*, 7456−7458. (l) Towatari, M.; Nishi, K.; Fujinami, T.; Matsumoto, N.; Sunatsuki, Y.; Kojima, M.; Mochida, N.; Ishida, T.; Re, N.; Mrozinski, J. *Inorg. Chem.* **2013**, *52*, 6160−6178. (m) Bhunia, A.; Yadav, M.; Lan, Y.; Powell, A. K.; Menges, F.; Riehn, C.; Niedner-Schatteburg, G.; Jana, P. P.; Riedel, R.; Harms, K.; Dehnend, S.; Roesky, P. W. *Dalton Trans.* **2013**, *42*, 2445−2450. (n) Chakraborty, A.; Bag, P.; Rivière, E.; Mallah, T.; Chandrasekhar, V. *Dalton Trans.* **2014**, *43*, 8921−8932. (o) Pasatoiu, T. D.; Etienne, M.; Madalan, A. M.; Andruh, M.; Sessoli, R. *Dalton Trans.* **2010**, *39*, 4802−4808. (p) Colacio, E.; Ruiz-Sanchez, J.; White, F. J.; Brechin, E. K. *Inorg. Chem.* **2011**, *50*, 7268−7273. (q) Mondal, K. C.; Kostakis, G. E.; Lan, Y.; Wernsdorfer, W.; Anson, C. E.; Powell, A. K. *Inorg. Chem.* **2011**, *50*, 11604−11611. (r) Okazawa, A.; Nojiri, H.; Ishida, T.; Kojima, N. *Polyhedron* **2011**, *30*, 3140−3144. (s) Sakamoto, S.; Fujinami, T.; Nishi, K.; Matsumoto, N.; Mochida, N.; Ishida, T.; Sunatsuki, Y.; Re, N. *Inorg. Chem.* **2013**, *52*, 7218−7229. (t) Zhao, L.; Wu, J.; Ke, H.; Tang, J. *Inorg. Chem.* **2014**, *53*, 3519−3525.

(11) (a) Hosoi, A.; Yukawa, Y.; Igarashi, S.; Teat, S. J.; Roubeau, O.; Evangelisti, M.; Cremades, E.; Ruiz, E.; Barrios, L. A.; Aromí, G. *Chem.—Eur. J.* **2011**, *17*, 8264−8268. (b) Peng, J. B.; Zhang, Q. C.; Kong, X. J.; Ren, Y. P.; Long, L. S.; Huang, R. B.; Zheng, L. S.; Zheng, Z. *Angew. Chem., Int. Ed.* **2011**, *50*, 10649−10652. (c) Peng, J. B.; Zhang, Q. C.; Kong, X. J.; Zheng, Y. Z.; Ren, Y. P.; Long, L. S.; Huang, R. B.; Zheng, L. S.; Zheng, Z. *J. Am. Chem. Soc.* **2012**, *134*, 3314−3317. (d) Wang, P.; Shannigrahi, S.; Yakovlev, N. L.; Hor, T. S. A. *Chem.—Asian J.* **2013**, *8*, 2943−2946. (e) Li, Z. Y.; Zhu, J.; Wang, X. Q.; Ni, J.; Zhang, J. J.; Liu, S. Q.; Duan, C. Y. *Dalton Trans.* **2013**, *42*, 5711−5717. (f) Pineda, E. M.; Tuna, F.; Zheng, Y.-Z.; Winpenny, R. E.; McInnes, E. J. *Inorg. Chem.* **2013**, *52*, 13702−13707. (g) Wang, P.; Shannigrahi, S.; Yakovlev, N. L.; Hor, T. S. *Dalton Trans.* **2014**, *43*, 182−187. (h) Das, S.; Dey, A.; Kundu, S.; Biswas, S.; Mota, A. J.; Colacio, E.; Chandrasekhar, V. *Chem.—Asian J.* **2014**, *9*, 1876−1887. (i) Upadhyay, A.; Komatireddy, N.; Ghirri, A.; Tuna, F.; Langley, S. K.; Srivastava, A. K.; Sañudo, E. C.; Moubaraki, B.; Murray, K. S.; McInnes, E. J.; Affronte, M.; Shanmugam, M. *Dalton Trans.* **2014**, *43*, 259−266.

(12) (a) Pardo, E.; Ruiz-García, R.; Cano, J.; Ottenwaelder, X.; Lescouëzec, R.; Journaux, Y.; Lloret, F.; Julve, M. *Dalton Trans.* **2008**, *21*, 2780−2805. (b) Palacios, M. A.; Rodríguez-Diéguez, A.; Sironi, A.; Herrera, J. M.; Mota, A. J.; Cano, J.; Colacio, E. *Dalton Trans.* **2009**, *40*, 8538−8547. (c) Colacio, E.; Palacios, M. A.; Rodríguez-Diéguez, A.; Mota, A. J.; Herrera, J. M.; Choquesillo-Lazarte, D.; Clérac, R. *Inorg. Chem.* **2010**, *49*, 1826−1833.

(13) Zeyrek, C. T.; Elmali, A.; Elerman, Y.; Svoboda, I. *Z. Naturforsch.* **2005**, *60b*, 143−148.

(14) *APEX2*; Bruker AXS: Madison, WI, 2010.

(15) *SAINT, Version 8.30a*; Bruker AXS: Madison, WI, 2013.

(16) Sheldrick, G. M. *SADABS, Version 2004/1*; Bruker AXS: Madison, WI, 2008.

(17) Sheldrick, G. M. *Acta Crystallogr., Sect. A: Found. Crystallogr.* **2008**, *64*, 112−122.

(18) Dolomanov, O. V.; Bourhis, J.; Gildea, R. J.; Howard, J. A. K.; Puschmann, H. *J. Appl. Crystallogr.* **2009**, *42*, 339−341.

(19) Clarke, B.; Clarke, N.; Cunningham, D.; Higgins, T.; McArdle, P.; Cholchúin, M. N.; O'Gara, M. *J. Organomet. Chem.* **1998**, *559*, 55−64.

(20) Llunell, M.; Casanova, D.; Cirera, J.; Bofill, J. M.; Alemany, P.; Alvarez, S.; Pinsky, M.; Avnir, D. *SHAPE v1.1b*; Barcelona, Spain, 2005.

(21) (a) Yamaguchi, T.; Sunatsuki, Y.; Kojima, M.; Akashi, H.; Tsuchimoto, M.; Re, N.; Osa, S.; Matsumoto, N. *Chem. Commun.* **2004**, 1048−1049. (b) Igarashi, S.; Kawaguchi, S.; Yukawa, Y.; Tuna, F.; Winpenny, R. E. P. *Dalton Trans.* **2009**, *17*, 3140−3142. (c) Cristóvao, B.; Pelka, R.; Miroslaw, B.; Klak, J. *Inorg. Chem. Commun.* **2014**, *46*, 94−97.

(22) (a) Feltham, H. L. C.; Lan, Y.; Klöwer, F.; Ungur, L.; Chibotaru, L. F.; Powell, A. K.; Brooker, S. *Chem.—Eur. J.* **2011**, *17*, 4362−4365. (b) Bi, Y.; Guo, Y.-N.; Zhao, L.; Guo, Y.; Lin, S.-Y.; Jiang, S. D.; Tang, J.; Wang, B. W.; Gao, S. *Chem.—Eur. J.* **2011**, *17*, 12476−12481 and references therein. (c) Ruiz, J.; Mota, A. J.; Rodríguez-Diéguez, A.; Titos, S.; Herrera, J. M.; Ruiz, E.; Cremades, E.; Costes, J. P.; Colacio, E. *Chem. Commum.* **2012**, *48*, 7916−7918.

(23) Bhunia, A.; Gamer, M. T.; Ungur, L.; Chibotaru, L. F.; Powell, A. K.; Lan, Y.; Roesky, P. W.; Menges, F.; Riehn, C.; Niedner-Schatteburg, G. *Inorg. Chem.* **2012**, *51*, 9589−9597.

(24) Chandrasekhar, V.; Bag, P.; Kroener, W.; Gieb, K.; Müller, P. *Inorg. Chem.* **2013**, *52*, 13078−3086.

(25) Rinehart, J. D.; Fang, M.; Evans, W. I.; Long, J. R. *Nat. Chem.* **2011**, *3*, 538−542.

(26) Ungur, L.; Thewissen, M.; Costes, J.-P.; Wernsdorfer, W.; Chibotaru, L. F. *Inorg. Chem.* **2013**, *52*, 6328−6337.

(27) Chilton, N. F.; Anderson, R. P.; Turner, L. D.; Soncini, A.; Murray, K. S. *J. Comput. Chem.* **2013**, *34*, 1164−1175.

(28) Boca, R. *Coord. Chem. Rev.* **2004**, *248*, 757−815.

(29) Singh, K.; Tibrewal, N. K.; Rajaraman, G. *Dalton Trans.* **2011**, *40*, 10897−10906 and references therein.

(30) Paital, A. R.; Mitra, T.; Ray, D.; Wong, W. T.; Ribas-Ariño, J.; Novoa, J. J.; Ribas, J.; Aromí, G. *Chem. Commun.* **2005**, *41*, 5172−5174.

(31) (a) Hou, Y.-L.; Xiong, G.; Shi, P.-F.; Cheng, R. R.; Cui, J.-Z.; Zhao, B. *Chem. Commum.* **2013**, *49*, 6066−6068. (b) Lorusso, G.; Sharples, J. W.; Palacios, E.; Roubeau, O.; Brechin, E. K.; Sessoli, R.; Rossin, A.; Tuna, F.; McInnes, E. J. L.; Collison, D.; Evangelisti, M. *Adv. Mater.* **2013**, *25*, 4653−4656. (c) Sibille, R.; Mazet, T.; Malaman, B.; François, M. *Chem.—Eur. J.* **2012**, *18*, 12970−12973.

(32) Guo, F.-S.; Chen, Y.-C.; Liu, J.-L.; Leng, J.-D.; Meng, Z. S.; Vrábel, P.; Orendáč, M.; Tong, M.-L. *Chem. Commun.* **2012**, *48*, 12219−12221.